ACI STRUCTURAL JOURNAL TECHNICAL PAPER

Title no. 97-S27

Analysis of Concrete Beams with Partially Bonded Composite Reinforcement

by Janet M. Lees and Chris J. Burgoyne

Beams prestressed with partially bonded fiber-reinforced plastic (FRP) tendons have high strength and rotation capacity but cannot be modeled by conventional techniques. Herein, it is assumed that all deformation takes place at cracks between rigid bodies. By setting up appropriate compatibility and equilibrium equations, the behavior at a single crack can be modeled, which then allows predictions to be made as to which of four possible events will occur next. These lead either to beam failure, or to changes in the geometry that can be analyzed using the same techniques. Comparisons are made with test results, and reasonable agreement is shown.

Keywords: beams (supports); bonding; composite construction; fibers (reinforcing materials); rigidity.

INTRODUCTION

Beams prestressed with fiber-reinforced plastic (FRP) rods behave differently from beams with steel. The tendons do not exhibit plasticity, but have high strain capacity. If tendons are fully bonded, they will tend to snap at the maximum load, while if unbonded, high moment capacity will not be achieved and the tendons will be used inefficiently.

To overcome these problems, it was proposed that beams should be made with partially bonded tendons.[1] This can be achieved either by having alternately bonded and unbonded regions, or by coating the tendons with a resin of known low shear strength. The results of an experimental study have already been published by ACI,[2] in which it was shown that moment capacities as good as those with bonded tendons could be achieved, but with rotation capacities in excess of those achievable with unbonded tendons.

The problem remains, however, that a method of analysis is required. A conventional analysis, based on strain compatibility and plane sections remaining plane, is not valid, as the tendon can move relative to the adjacent concrete. Nor do the methods used to analyze unbonded tendons work because the movement of the tendon is restrained. Thus, a more rigorous analysis is presented herein. It is compared with experimental results for beams with aramid fiber tendons, but the principles are more generally applicable and could be used as the basis of a design method.

RESEARCH SIGNIFICANCE

FRPs do not yield, and a large rotation capacity is desirable for FRP prestressed concrete beams. Furthermore, because FRPs are generally more expensive than steel, it is important that they are used efficiently.

Conventional design methods do not give optimal results for FRP prestressed structures, and the use of partially bonded tendons represents a more rational design basis for these novel materials.

This study provides an analytical basis that can be used to predict the performance of beams with partially bonded FRP tendons. The analysis highlights key events and design parameters that dictate the behavior of these novel members.

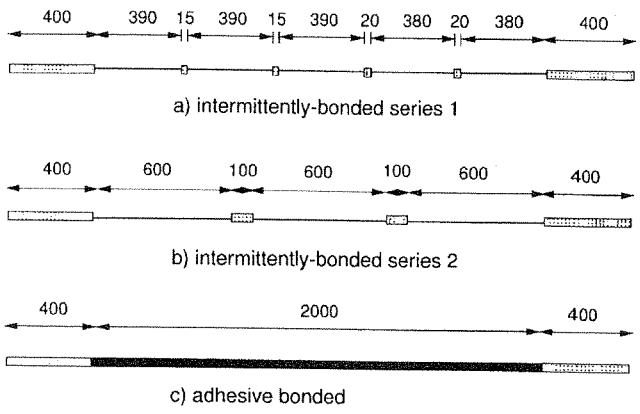

Fig. 1—Tendon details.

EXPERIMENTAL STUDY

In the experimental study,[2] pretensioned concrete beams with either fully bonded, unbonded, or partially bonded FRP tendons were tested. The partial bonding was achieved in one of three ways, as shown in Fig. 1. Intermittently bonded (IB) tendons were made by alternately bonding and debonding lengths of tendon. In the IB Series 1 beams, the bonded lengths were very short and were designed to slip before the beam failed; in the IB Series 2 beams, the bonded lengths were designed not to fail. Adhesively bonded beams were made by coating the tendon, away from the anchorage zone, in a resin of low shear strength. Fully bonded and unbonded beams were also tested, but are not described herein.

The beams were 2800 x 200 x 100 mm, and had either three 3.7 mm FiBRA tendons or two 4 mm Technora tendons, both of which are made from aramid fibers (Table 1). The tendons were pretensioned to approximately 65% of the tendon failure load. The beams were loaded in four-point bending; the clear span was 2400 mm, and the constant moment region was 800 mm long.

ANALYSIS BASED ON STRAIN COMPATIBILITY

The behavior up to first cracking can be modeled by a conventional strain compatibility approach that also works up to failure for fully bonded beams. For the partially bonded beams, however, after cracking, the beam is modeled by as-

ACI Structural Journal, V. 97, No. 2, March-April 2000.
MS No. 98-264 received July 22, 1998, and reviewed under Institute publication policies. Pertinent discussion will be published in the January-February 2001 *ACI Structural Journal* if received by September 1, 2000.

Janet M. Lees *is a lecturer at the University of Cambridge, UK. She received her PhD in 1997 from the University of Cambridge. Her research interests include the use of fiber-reinforced plastics in construction applications, and the behavior of concrete structures.*

ACI member **Chris J. Burgoyne** *is a reader at the University of Cambridge. He is a member of ACI Committee 440, Fiber-Reinforced Polymer Reinforcement. His research interests include advanced composites applied to concrete structures.*

Table 1—Tendon and fiber materials properties[3-7]

Material	Density, kg/m^3	Fiber type	Young's modulus, GPa	Maximum elongation, %	Tensile strength, MPa	V_f, %
FiBRA rod	1.28	Kevlar 49	68.6	2.0	1480	65 to 70
Kevlar 49 fiber	1.45	N/A	120.0	2.5	2800	N/A
Technora rod	1.30	Technora	54.0	3.7	1900	65
Technora fiber	1.39	N/A	73.0	4.6	3400	N/A
Steel (high yield)	7.80	N/A	200	10.0	650	N/A
Steel (prestress)	7.80	N/A	220	4.2*	1760	N/A

*Measured value.

suming that it behaves as a series of rigid blocks, which matches the experimental observation that most of the rotation takes place at a relatively small number of crack locations (Fig. 2). Thus, the aim is to set up the relevant equilibrium and compatibility conditions at each crack. The process will be described in detail for a single crack; extension to multiple cracks is then straightforward.

Mathematical basis for rigid body analysis with single crack

In Fig. 3, the beam behavior is modeled as two rigid blocks connected at a crack location 1. The deflection of the beam at the crack location δ_{cr1} represents the movement relative to the original horizontal profile of the beam.

At the crack opening, the rotation is deemed to occur about the neutral axis, which is at a depth *nd*. The concrete above the neutral axis is in compression, and the extensions in the tendon are compatible with the crack opening. The total extension due to the rotation δL_θ is

$$\delta L_\theta = \delta L_{\theta 1} + \delta L_{\theta 2} = 2d(1-n)\sin\left(\frac{\theta_1 + \theta_2}{2}\right) \quad (1)$$

The components of the tendon force in the x and y directions that rotate with the blocks F_{tx} and F_{ty} are related to F, which is the force in the section of tendon that spans the crack (Eq. (2) and (3)).

$$F_{tx} = F\cos\left(\frac{\theta_1 + \theta_2}{2}\right) \quad (2)$$

$$F_{ty} = F\sin\left(\frac{\theta_1 + \theta_2}{2}\right) \quad (3)$$

The distribution of the force in the concrete compressive zone can be approximated as a rectangular stress block[8] (Fig. 4) as the concrete approaches its ultimate limit state. Immediately after cracking, the concrete is still likely to be elastic and hence, this type of plastic stress distribution is not appropriate. With

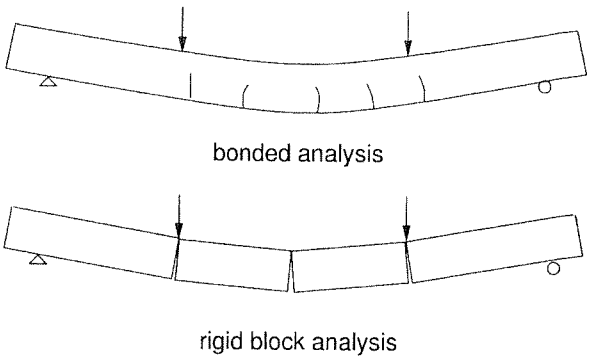

Fig. 2—Schematic comparison of bonded analysis and rigid block analysis.

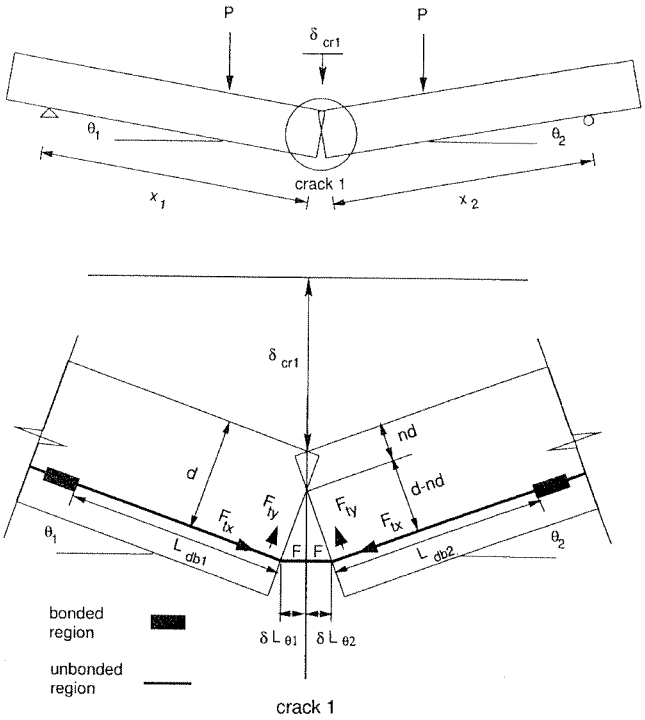

Fig. 3—Geometry of rigid block rotation.

further loading and with the onset of large strains, however, this model is reasonable.

The force in the concrete F_{cx} is then given by

$$F_{cx} = (0.67f_{cu})b(0.9nd) \quad (4)$$

Axial equilibrium requires

$$F_{tx} = F_{cx} \quad (5)$$

If the force F_{tx} is known, the tendon extensions δL_{Fx1} and δL_{Fx2}, due to the increase in the force in the tendon relative to the initial prestress level $F_{tx} - P_o$, can then be calculated by considering the debonded lengths over which the tendon is free to extend L_{db1} and L_{db2} (Fig. 3).

The sum of these extensions, δL_F, (Eq. (6)) can be equated to the extensions predicted using Eq. (1)

$$\delta L_F = (\delta L_{Fx1} + \delta L_{Fx2})\cos\left(\frac{\theta_1 + \theta_2}{2}\right) \quad (6)$$

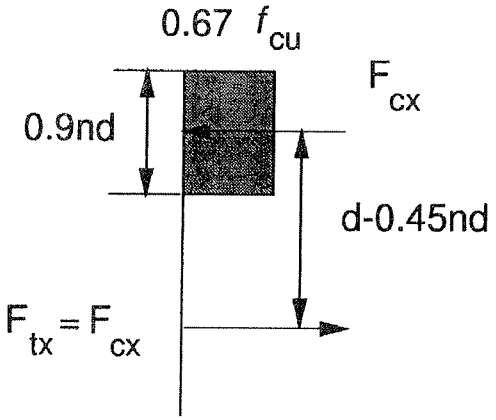

Fig. 4—Distribution of force in concrete: rectangular stress block.

$$= \frac{(F_{tx} - P_o)}{E_t A_t}(L_{db1} + L_{db2})\cos\left(\frac{\theta_1 + \theta_2}{2}\right)$$

It is of note that for small rotations, the cosine terms in Eq. (2) and (6) will be approximately equal to 1.

Numerical procedure

Using the equations and assumptions of the previous section, a numerical procedure can be formulated to calculate the deflection profile of a beam for a given loading. The two primary variables are chosen to be the deflection at the crack location δ_{cr1} and the depth of the neutral axis *nd*.

If the crack location, and hence the distances x_1 and x_2, are known, then for any particular value of δ_{cr1}, the angles θ_1 and θ_2 are determinate.

The procedure can be summarized as follows:

- Assume value of δ_{cr1};
- Find θ_1 and θ_2;
- Iterate *nd* until $\delta L_F = \delta L_\theta$;
- Determine applied moment and loads; and
- Repeat with new value of δ_{cr1}.

Possible next events

The starting point for the rigid body analysis is that the first central crack has already occurred. After first cracking, the load is increased until one of several things happens:

1. The concrete will crush if the angle of rotation at the hinge location becomes excessive. A large rotation induces high localized strains in the concrete, and results in the failure of the concrete;
2. The tendons will rupture if the strain in the tendon is greater than the extension capacity of the FRP;
3. The bond in a segment will break down if the forces to be transmitted through the segment exceed the bond capacity of the region; and
4. Another crack will form if the tensile stress buildup along the bottom face of the beam exceeds the tensile capacity of the concrete.

The occurrence of either Event 1 or 2 will result in the failure of the beam. Events 3 and 4, however, can occur at various stages of loading.

Bond breakdown

Detailed models have been proposed to describe the bond stress-slip behavior of reinforcement being pulled out of a block of concrete. In particular, the Comité EuroInternational du Béton (CEB) Model Code[9] suggests that the variation of bond stress with slip can be described using a curve that consists of four parts (Fig. 5). Note that the CEB model is based on

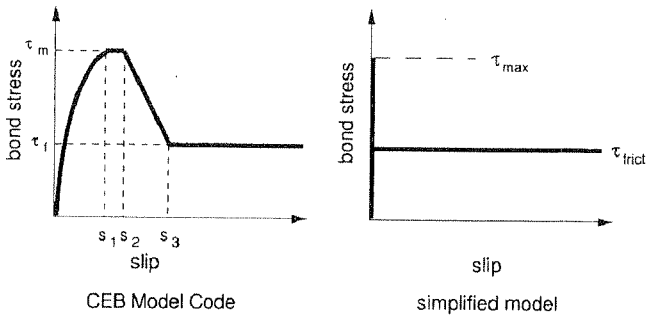

Fig. 5—Schematic shear stress versus slip curves.

the pullout behavior of steel reinforcement, and the mechanisms involved are likely to differ when FRP rods are used. Others,[10,11] however, have found that the model adequately describes the bond slip behavior of some FRP rods.

In the present analysis, the treatment of bond is somewhat simplified (Fig. 5). In the ascending branch of the shear stress-displacement curve, it is assumed that no slip occurs up to a maximum shear stress of τ_{max}. As the bond breaks down, the shear stress drops to τ_{frict}, remaining constant with increasing slip.

This simplified model is justified because large slips are expected in the current work. Hence, the magnitude of slip that occurs prior to the bond breaking down will be small in comparison with the slip that will occur once only the frictional bond strength remains.

A further assumption is that the bond stress does not vary along the length of the bonded region. Hence, $\tau = b_1$ where b_1 is a constant. As the bond stress is taken to be constant, the maximum force F_{max} that can be transmitted through the bonded region of length L_b prior to bond breaking down is the product of the maximum shear stress and the embedded surface area of the tendon

$$F_{max} = 2\pi r L_b \tau_{max} \quad (7)$$

If the force to be carried by the bonded segment exceeds F_{max}, then the bond breaks down and only a frictional bond resistance remains. Furthermore, large extensions occur through the region. As the shear stress τ_{frict} is assumed to stay constant with increasing displacements, then the force transmitted through the bonded length F_{frict} does not vary, so that

$$F_{frict} = 2\pi r L_b \tau_{frict} \quad (8)$$

Generalized analysis procedure

For the intermittently bonded beams, a closed-form solution for the force in terms of the deflection can be found. In the initial configuration the beam is subdivided into two halves, with the centerline as the origin.

A schematic representation of how the forces in the tendon along the length of a beam can vary can be found in Fig. 6. In this figure, the left-hand side of a beam with a total of 23 segments is portrayed. Prior to loading, the force in the tendon segments is the initial prestress force P_o. As the applied load increases, however, the forces in the tendon segments alter.

For the purposes of illustration, it will be assumed that for this particular combination of load F and rotation θ_1, the bond in Segments 9 and 11 has broken down, and the frictional bond force is transmitted through these regions. The integrity of the bond in Segment 7 is maintained (hence, $T_8 - T_6 \leq F_{max}$), although bond forces are transmitted through the region.

For small rotations, the tendon forces in the unbonded segments on the left-hand side of the beam can be calculated as follows

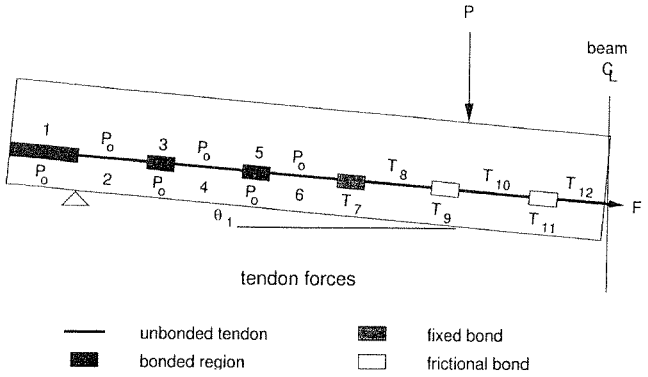

Fig. 6—Schematic representation of forces along length of tendon.

$$T_{12} = F$$

$$T_{10} = T_{12} - F_{fricl}$$

$$T_8 = T_{10} - F_{fricl}$$

$$T_6 = P_o$$

etc.

The force of the odd-numbered segments T_{11}, T_9, T_7, etc., is taken to be the average of the force on either side of the segment under consideration.

In these equations, the frictional forces and the initial prestress are known. All the remaining forces along the length of the tendon can be found in terms of the force T_{12} in the centerline Segment 12.

The overall extension of the tendon is then

$$\delta L_F = \sum_{j=8}^{12} \frac{(T_j - P_o)L_j}{E_t A_t} \quad (9)$$

Further cracking—Buildup of stresses along bottom face

After the first cracking has occurred, a knowledge of the buildup of stresses along the bottom face of the beam is necessary to ascertain where the next crack will form. To determine the stresses on the bottom surface, a detailed analysis of the concrete is required; an analysis based solely on stress resultants is insufficient because the local effects of the loads need to be considered. A beam model was formulated, and both a theoretical analytical solution and a finite element solution were investigated.

Analysis model—Figure 7 shows the forces acting on the concrete in 1/2 of a typical beam. These forces can be approximated by four separate loads acting on a cantilever, where the free end of the cantilever is analogous to the central crack face. The four loading components represent:

1. An eccentric point load normal to the end of a cantilever (to model the concrete compressive force);
2. A load acting at right angles to the top face of the cantilever (the applied load);
3. The combination of a vertical force applied at the tendon level, and an equal and opposite force in the concrete compression zone applied at the end of the cantilever (to account for the vertical component of the tendon force F_{ty}) (Fig. 3); and
4. Internal point loads acting at the tendon depth (to simulate the bond forces applied to the concrete).

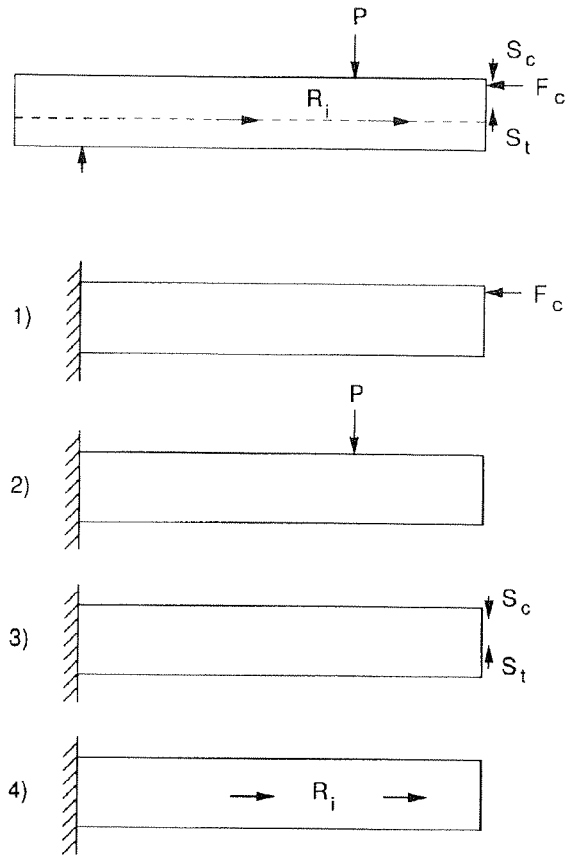

Fig. 7—Forces acting on beam.

The fixed end of the cantilever does not reflect the actual support conditions, but this is not of concern because the applied loadings and internal forces will be in equilibrium. Superposition of the factored unit load case results will therefore result in a solution with no moment at the support. As there is no net moment at the left-hand end, the effect of the clamped end in each of the individual analyses is, by St. Venant's principle, not significant near the far end of the cantilever when the four load cases are combined.

Theoretical analytical solution—Although it was known that a finite element analysis could be performed, an analytical solution would have been preferable. Exact solutions, however, only exist for an eccentric point load,[12,13] and they are extremely complex.

Finite element solution—An analysis using a finite element (FE) package was therefore carried out to determine the tensile stress buildup along the base of the beam.

It was found that the tensile stresses induced as a result of the vertical component of the tendon force (loading Component 3) were small and have been neglected.

The FE analysis showed that the most significant variations in stress at the bottom face were typically localized to within a region close to the point of the load application, as would be expected by St. Venant's principle. This effect was particularly noticeable in the concrete compressive force results.

The combined effect of the loading components on the tensile stress buildup will be determined in conjunction with the analysis at the crack. If the stress at a particular location along the length of the beam exceeds the tensile capacity of the concrete, a crack will occur.

Generalization of formulation to multiple cracks

If further cracking occurs, the procedures outlined previously can be generalized to consider the case where multiple cracks form under a given load condition (Fig. 8). If the location of

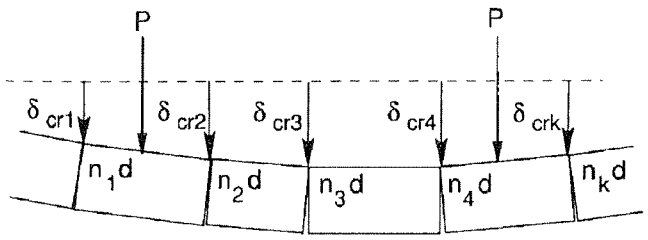

Fig. 8—Diagram of multiple cracking behavior.

each new crack is known, then the deflection at the crack locations δ_{cr} is assumed. Using the assumed deflection profile, the neutral axis depth nd is then iterated until a solution is found that satisfies both the equilibrium and compatibility criteria (hereafter referred to as an equilibrium/compatibility solution). If no solution is found, then the assumed deflection profile is revised and the procedure repeated.

It is possible that there is more than one combination of deflection profile and neutral axis depth that would result in an equilibrium/compatibility solution; this should be considered for complex load histories.

If several cracks occur in a constant moment region, the force in the tendon spanning each crack must be the same. This feature was incorporated in the current analysis to simplify the computation. In the majority of the experimental beams, the cracks did occur in the constant moment region, and hence, the assumption was valid. If this is not the case, however, refinements to allow for the varying compression and tension can be provided.

Additional repercussions of multiple cracking

Bond stress direction—If a bonded region is located between two cracks, then the region will be loaded from both directions; the behavior depends on the bond state of the region prior to the occurrence of the second crack.[14]

Tensile stress distribution—The buildup of concrete tensile stress along the bottom face of a block bounded by two cracks also changes. The resulting stress distribution depends on the length of the block, the force in the concrete, and the status of any bonded segments within the block. In the results presented herein, it has been assumed that a further crack would not occur in such a block.

Computer program

A computer program was written to carry out the rigid body analysis. The input data include the bond characteristics of the tendons and the details of the bonded and unbonded regions. Data files for the unit load cases, which correspond to the buildup of tensile stresses along the bottom face of the beam, are generated using the FE program. The program calculates the first cracking moment using a strain compatibility approach, and then the iterative calculations commence.

The debonded length L_{db} reflects the distance between the outermost segments in which the bond has not broken down. For a set debonded length, the angle between the rigid blocks θ is incremented between the limits θ_{min} and θ_{max}; for each value of θ, the neutral axis depth nd is also incremented. The forces in the tendon and the concrete are calculated and checked for both axial force and moment equilibrium.

If an equilibrium/compatibility solution does not exist, then θ is incremented, and the process repeated. Conversely, when a solution has been found, the forces along the tendon are updated. The force in the tendon at the beam centerline is known from the previous step, and hence, the forces along the tendon can be calculated.

If the force in the tendon T is found to be equal to the failure load P_{ult}, then tendon rupture occurs and the program is terminated. Otherwise, the forces transmitted through the bonded lengths are checked. If the forces exceed the bond capacity of a region, the bond is deemed to have broken down. If this is the case, then L_{db} is increased and the loop repeated.

If the bond does not break down, the tensile stresses along the bottom face of the beam are checked to see if cracking occurs. If a crack does form, the status of the bond in the adjacent bonded regions and the forces in the tendon lengths next to the crack locations are adjusted, and the process of checking for an equilibrium/compatibility solution, bond breakdown, and cracking is repeated.

Table 2—Bond parameters used in analysis of beams

Material	Adhesive coating	τ_{max}, MPa	τ_{frict}, MPa
Technora	n	20	14
FiBRA	n	11	8
Technora	y	2.1	1.1
FiBRA	y	0.7	0.5

DISCUSSION

A comparison was made between the analytical and experimental results. The results for an intermittently bonded FiBRA beam from Series 1, an intermittently bonded Technora beam from Series 2, and an adhesive bonded FiBRA beam are presented as follows.

Input parameters

The input values for the bond parameters τ_{max} and τ_{frict} for both the adhesive coated and uncoated tendons[4,15] are shown in Table 2. The concrete compressive cube and tensile modulus of rupture strength were approximately 56 and 3.3 MPa, respectively.

Intermittently bonded—Series 1

This series of beams was designed so that the load would break down as the load increased. A graph of the relationship between the applied load and rotation can be found in Fig. 9. Bond breakdown and concrete cracking events are noted.

Both the experimental and predicted crack locations can be found in Table 3. The predicted tensile stresses along the bottom face of the beam often showed little variation near the maximum, so a range of locations have been included in the table.

In general, the correlation between the experimental and analytical results for the first series of intermittently bonded beams was quite good. The second and third crack locations were within the predicted range (Table 3). The slopes of the predicted load-versus-θ curves, however, are slightly lower than the experimental curves. This is probably due to the analytical concrete model that ignores concrete elasticity after cracking.

Tendon rupture, based on the manufacturer's assured strength rather than measured strength, was expected in the beam at a rotation of approximately 0.12 radians (in tests described elsewhere,[16] the measured strength of the tendon was found to be 15% higher than the assured strength). In the experimental beam, the concrete started to fail at a rotation between 0.12 and 0.13 radians.

Intermittently bonded—Series 2

This series of beams was designed so that bond breakdown would not occur. A typical comparison is shown in Fig. 10.

The correlation between the experimental and analytical results is not as good as for the Series 1 beams. The load and rotation at which second cracking occurred are in agreement with the experiments. For the third crack, however, the predicted rotation is greater than the experimental value, and the

Table 3—Crack locations for partially-bonded beams*

Beam identification	Experimental		Predicted	
	Crack 2	Crack 3	Crack 2	Crack 3
Intermittently-bonded Series 1	1560	830	1500 to 1600	800 to 900
Intermittently-bonded Series 2	1720	730	1550 to 1650	750 to 850
Adhesive bonded	840	1550	840	1560

*Distance in mm from left hand support.

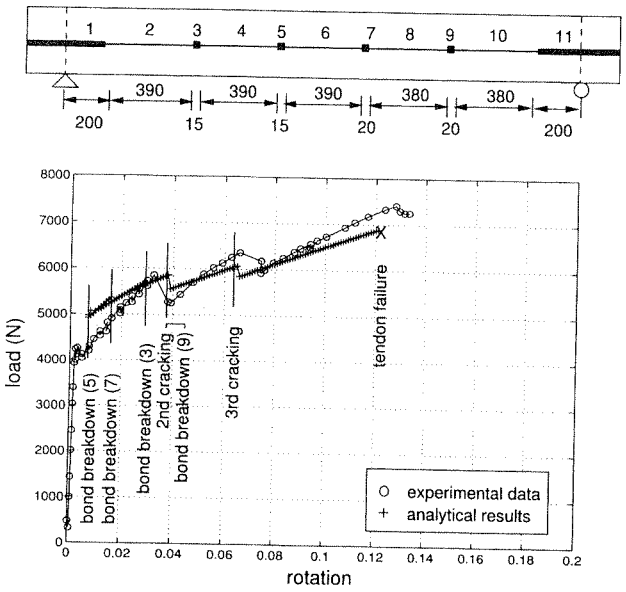

Fig. 9—Load-deflection curves: intermittently-bonded Series 1.

cracking load was underestimated. The analytical model predicts that failure would occur due to tendon rupture. In the experimental beam, failure was due to a combination of concrete crushing and tendon rupture, which appeared to occur simultaneously.

The Series 2 beams are not as sensitive to the values of τ_{max} and τ_{frict} as the Series 1 beams.

In the experiments, the third crack occurred at a higher load than the second crack. In theory, if the bond does not break down and the bonded and unbonded segments are symmetrical about the beam centerline, both cracks should occur at a similar load. The experimental crack locations are up to 120 mm outside the constant moment region, which also contradicts the theoretical prediction. This is probably due to the extensive horizontal cracking on either side of the central crack location during testing. It is expected that horizontal cracking will affect not only the crack location, but also the cracking load and the rotation at which cracking occurs.

If cracks occur outside the constant moment region, then the forces in the tendon lengths spanning the cracks are not equal to the centerline tendon force as assumed, so the program will underestimate the load at which a particular rotation will occur.

Adhesive bonded

In Fig. 11, the theoretical and experimental results for an adhesive-bonded beam are compared. The length of the adhesive-bonded tendons was arbitrarily treated as a series of 100 mm bonded tendon segments, and it is predicted that there is an extensive breakdown of bond throughout testing.

The slopes of the predicted curves coincide fairly well with the experimental results. According to the computer analysis,

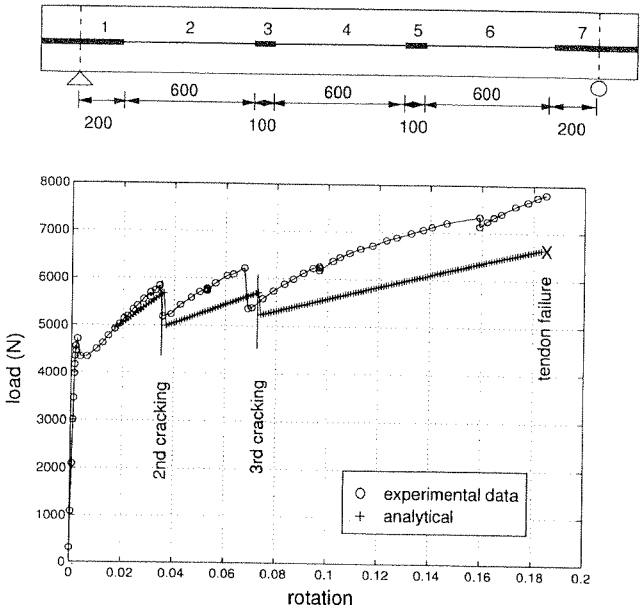

Fig. 10—Load-deflection curves: intermittently-bonded Series 2.

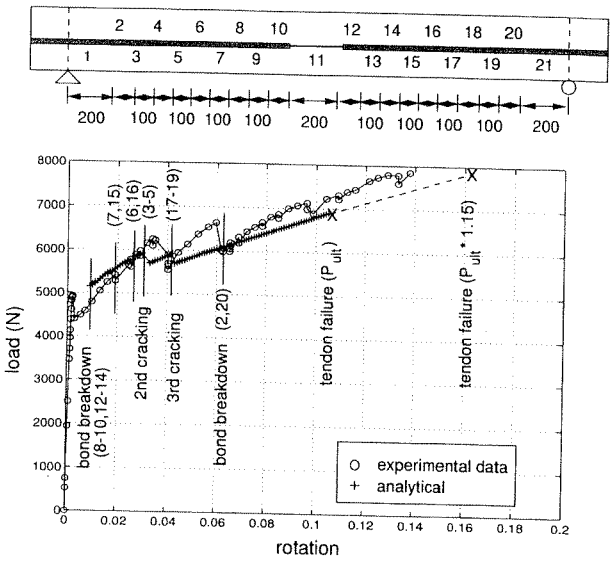

Fig. 11—Load-rotation curves: adhesive bonded.

the beam should have failed due to tendon rupture at a load of close to 7000 N. The computer program predicts failure based on the manufacturers' assured loads P_{ult} for the tendons. If the ultimate load capacity of the tendons is taken to be the measured tendon strength, then a tendon failure would not occur until approximately 8000 N, as observed.

Extensions/limitations of program

The program was written specifically to elucidate the behavior of the experimental beams. This type of analysis, however, could be extended to include more general applications: a more refined bond stress-slip relationship could be incorporated; multiple tendon layers could be treated more rigorously, and the FE results could be nondimensionalized and linearized so that specific FE runs would not be needed for each new structure.

Other additions would be to incorporate a concrete model that reflects the load history and the transition from the elastic

to the elastoplastic to the fully plastic state. There is, however, the question of how to translate the displacements in the concrete that are calculated from the rigid body geometry into actual concrete strains. To do so, the length of the region of concrete over which the displacement occurs is required, and this value is unknown.

A constraint within the program is the assumption that the cracks occur inside the constant moment region. As evident even in the work presented herein, this assumption is not always valid. The evaluation of the tendon force at a crack location outside the constant moment region is not problematic. The difficulty lies in the determination of the angles between the blocks. If the bond has not broken down, then certain inferences about the angles between the blocks can be made. If the bond does break down, however, the distribution of the angles remains indeterminate, and a solution can only be found by iterating through possible deflection profiles.

CONCLUSIONS

A simplified analysis, based on rigid body rotations of blocks between cracks, which satisfies both equilibrium of forces and compatibility of geometry, has been shown to model reasonably accurately the postcracking behavior of partially bonded beams, and to allow the prediction of both failure loads and corresponding rotations. It is suggested that this type of analysis could be used to produce design guidelines.

ACKNOWLEDGMENTS

The authors are grateful for the support of Teijin Ltd. and Mitsui Construction Co. Kevlar is a trade name of Du Pont, Technora of Teijin, and FiBRA of Mitsui. One of the authors (JML) was sponsored by the Natural Sciences and Engineering Research Council of Canada (NSERC), and is appreciative of NSERC's financial assistance.

NOTATIONS

A_t = area of tendon
b = beam width
b_1 = constant
d = effective depth of beam
E_t = modulus of elasticity of tendon
f_{cu} = concrete compressive cube strength
f_t' = tensile strength of concrete inferred from cylinder strength
F = tendon force
F_c = concrete compressive force
F_{cx} = component of concrete force in x-direction
F_{frict} = frictional bond force that can be carried by region
F_{max} = maximum force carried by bonded region
F_{tx} = component of tendon force in x-direction
F_{ty} = component of tendon force in y-direction
j = segment reference number
k = crack number
L_b = bonded segment length
L_{db} = debonded length of tendon
nd = neutral axis depth
P = applied load
P_o = initial prestress force
P_{ult} = manufacturer's assured load for tendon
r = tendon radius
R_i = tendon bond forces
s_1, s_2, s_3 = values of slip
S_c, S_t = vertical forces transmitted to concrete
T = force in tendon segment
V_f = volume fraction of fibers
x = distance from end of specimen
δ_{cr} = deflection at particular crack
δL_F = total tendon extension due to Force F
δL_θ = total tendon extension due to Rotation θ
θ = angle of rotation
θ_{min}, θ_{max} = rotation limits
τ = bond shear stress
τ_f, τ_{frict} = frictional bond stress
τ_m, τ_{max} = average maximum bond shear stress

REFERENCES

1. Burgoyne, C. J., "Should FRP be Bonded to Concrete?" *Fiber Reinforced Plastic Reinforcement for Concrete Structures International Symposium*, SP-138, A. Nanni and C. W. Dolan, eds., American Concrete Institute, Farmington Hills, Mich., 1993, pp. 367-380.

2. Lees, J. M., and Burgoyne, C. J., "Experimental Study of Influence of Bond on Flexural Behavior of Concrete Beams Pretensioned with Aramid Fiber Reinforced Plastics," *ACI Structural Journal*, V. 96, No. 3, May-June 1999, pp. 377-385.

3. Mera, H., and Takata, T., "High-Performance Fibers," *Ullmann's Encyclopedia of Industrial Chemistry*, V. A13. VCH, 5th Edition, 1989.

4. Teijin Ltd., "High-Tenacity Aramid Fiber—Technora," *Technical Information*, TIE 05/89.11, 1989.

5. Tamura, T., "FiBRA." "Fiber Reinforced Plastic (FRP) Reinforcement for Concrete Structures: Properties and Applications," *Developments in Civil Engineering*, 42, A. Nanni, ed., Elsevier Science Publishers B.V., 1993, pp. 291-303.

6. Tanigaki, M.; Okamoto, T.; Tamura, T.; Matsubara, S.; and Nomura, S., "Study of Braided Aramid Fiber Rods for Reinforcing Concrete," *IABSE*, 13th Conference, Helsinki, 1988, pp. 15-20.

7. Kakihara, R.; Kamiyoshi, M.; Kumagai, S.; and Noritake, K., "A New Aramid Rod for the Reinforcement of Prestressed Concrete Structures," *Advanced Composites Materials in Civil Engineering Structures Proceedings*, Las Vegas, Jan. 31, 1991, MT Div/ASCE, pp. 132-142.

8. Hognestad, E.; Hanson, N. W.; and McHenry, D., "Concrete Stress Distribution in Ultimate Strength Design," ACI JOURNAL, *Proceedings* V. 27, No. 4, Dec. 1955, pp. 455-479.

9. Comité Euro-International du Béton, *Bulletin D'Information* No. 203, CEB-FIP Model Code 1990 Final Draft, Chapters 1-3, July 1991.

10. Faoro, M., "The Influence of Stiffness and Bond of FRP Bars and Tendons on Structural Behavior of Reinforced Concrete Members," *Advanced Composite Materials in Bridges and Structures: 2nd International Conference*, M. M. El-Badry, ed., The Canadian Society for Civil Engineering, Montreal, Quebec, Canada, Aug. 11-14, 1996, pp. 885-892.

11. Cosenza, E.; Manfredi, G.; and Realfonzo, R., "Bond Characteristics and Anchorage Length of FRP Rebars," *Advanced Composite Materials in Bridges and Structures: 2nd International Conference*, M. M. El-Badry, ed., The Canadian Society for Civil Engineering, Montreal, Quebec, Canada, Aug. 11-14, 1996, pp. 909-916.

12. Baker, G.; Pavlović, M. N.; and Tahan, N., "An Exact Solution to Two-Dimensional Elasticity Problem with Rectangular Boundaries under Arbitrary Edge Forces," *Philosophical Transactions of the Royal Society of London*, 343(A), 1993, pp. 307-336.

13. Tahan, N.; Pavlović, M. N.; and Kotsovos, M. D., "Single Fourier Series Solutions for Rectangular Plates under In-plane Forces, with Particular Reference to the Basic Problem of Colinear Compression—Part 1: Closed-Form Solution and Convergence Study," *Thin-Walled Structures*, 15, 1993, pp. 291-303.

14. Lees, J. M., "Flexure of Concrete Beams Pretensioned with Aramid FRPs," PhD thesis, Department of Engineering, University of Cambridge, UK, 1997.

15. Sheard, S., "Bond Characteristics and Stress-Slip Model for Aramid Fiber Reinforcement," fourth year project, Department of Engineering, University of Cambridge, UK, May 1996.

16. Lees, J. M.; Gruffydd-Jones, B.; and Burgoyne, C. J., "Expansive Cement Couplers—A Means of Pretensioning Fiber-Reinforced Plastic Tendons," *Construction and Building Materials*, V. 9, No. 6, 1995, pp. 413-423.